

# HIGH SPECTRAL RESOLUTION LIDAR AT THE UNIVERSITY OF WISCONSIN-MADISON

Ilya I. Razenkov, Edwin W. Eloranta

*University of Wisconsin-Madison, 1225 W. Dayton St., Madison, WI, 53706, USA, razenkov@wisc.edu*

## ABSTRACT

This paper describes the modifications done on the University of Wisconsin-Madison High Spectral Resolution Lidar (HSRL) that improved the instrument's performance. The University of Wisconsin HSRL lidars designed by our group at the Space Science and Engineering Center were deployed in numerous field campaigns in various locations around the world. Over the years the instruments have undergone multiple modifications that improved the performance and added new measurement capabilities such as atmospheric temperature profile and extinction cross-section measurements.

## 1 INTRODUCTION

High Spectral Resolution Lidars developed in the University of Wisconsin-Madison have proven to be eye-safe and capable of continuous operation in remote areas requiring low maintenance. In the last 8 years our group has developed and built five HSRL instruments in four different configurations. The instruments were successfully deployed in 18 field campaigns around the globe including remote locations such as McMurdo Station in Antarctica, and Barrow, Alaska. This paper describes the latest version of our most advanced HSRL lidar.

## 2 HIGH SPECTRAL RESOLUTION LIDAR SYSTEM

### 2.1 Lidar transmitter

The HSRL technique uses spectral information from the lidar returns which requires a narrow high spectral resolution laser (<100MHz) and ~10 GHz laser frequency tuning capability [1]. The transmitter consists of the injection seeded diode pumped Nd:YAG laser from Photonics Industries Inc. The laser emits two wavelengths 532 nm and 1064 nm and operates at 4000 Hz pulse repetition rate. The single mode DFB seed laser diode (1064 nm) from QD-Lasers is used to injection-seed the

host laser cavity. A custom controller was developed to provide a high frequency stability, smooth tuning, and good spectral purity of the laser. The host laser cavity end mirror is mounted on the piezo actuator and controlled by another custom-built controller. It adjusts the cavity length every four laser shots and tunes the cavity to the wavelength of the seed laser. The laser is tunable over 1 nm range at 1064 nm wavelength. The seed laser is injected into the host laser through a fast fiber-optic switch (~200 ns switching time) with two outputs. The switch is programmed to direct the light to the laser cavity ~10 ns before the host laser fires and switches off immediately after the laser pulse. The switch is implemented to avoid the amplification of the seed laser light. All the remaining time the fiber-optic switch directs the seed laser light to a second output, where the 1064 nm light is frequency doubled for use in the instrument calibration. The host laser cavity has a partially reflective mirror and an external KTP frequency doubling crystal mounted after the laser output coupler. KTP converts ~30% of the 1064nm light into the visible 532 nm light with the output power ratio ~700mW@532nm : 1400mW@1064nm.

The seed laser is frequency locked to the iodine absorption line #1109 using a frequency locking setup. The setup uses a 100 mm long iodine absorption cell and two energy monitors. The computer controlled DAQ applies voltage to the seed laser to control the frequency and does a slow frequency tuning of the laser. The laser cavity controller scans the host laser cavity end-mirror optimizing the cavity length to the resonant frequency, and measures the iodine line slope using the energy monitors' ratios (see Figure 1). The zero-slope corresponds to the peak absorption of the iodine line. The slope information is transferred to the computer providing an active feedback for frequency control. That allows the frequency locking accuracy of around ±15 MHz. The lidar transceiver parameters are summarized in Table 1.

*Table 1 HSRL parameters*

<b>Transmitter</b>	Laser Photonics Ind. Inc.	DS10-532/1064 SLM
	Wavelength	532/1064 nm
	Transmitted eye-safe power	0.2 Watt@532 0.6 Watt@1064
	Spectral width	<50MHz
	Spectral purity	1:5000
	Locking accuracy	30 MHz
	Pulse repetition rate	4 kHz
	Telescope Aperture	400 mm, Shared with receiver
	Transmitted beam divergence	~2 $\mu$ rad
<b>Receiver</b>	Scanning telescope	400 mm diam. Dall-Kirkham
	Narrow field-of-view	100 $\mu$ rad
	Wide field-of-view	1 mrad
	Spectral bandwidth	8 GHz
	Iodine filters (line #1109)	1.8 GHz (narrow iodine filter) 2.85 GHz (Argon broadened)
	Detectors	Geiger Mode APD SPCM-AQR-H-12

## 2.2 Optical design

In our HSRL instrument the transmitter and the receiver are located on opposite sides of the breadboard. The temperature difference of the breadboard skins can deform it and deflect the laser beam. Locating the optics on both sides of the breadboard compensates these beam deflection errors. The breadboard is positioned horizontally. The part of the transmitter's optics, along with frequency control optics and interferometer, are on the bottom side of the breadboard, and the receiver is on the top. The laser is mounted under the breadboard using a kinematic mount. Figure 1 shows the complete optical diagram of the High Spectral Resolution Lidar.

Some portion of the laser light is picked off from the beam by a wedge for locking setup, laser spectrum quality control and the interferometer. Then light passes through the glan polarizer and is expanded by the 10x beam-expanding telescope. The broadband non-polarizing beam splitter (R/T=65/35S) is used as a transceiver switch. Because the beamsplitter substrate is a 30 arcmin wedge, a compensating wedge is used to correct for beam's chromatic deflections due to glass dispersion at 532 and 1064 nm. The beamsplitter

enables a detection of both parallel- and cross-components of the lidar returns and allows to alternate the polarization of the transmitted light pulses using a Pockels cell in the transmitter. It improves calibration of the cross-polarized channel and simplifies the optics alignment.

An achromatic half-wave plate is mounted on the telescope motor with a 1:2 gear reduction mechanism. It is used to compensate for the rotation of a polarization plane during telescope rotation. Then, the beam is further expanded by 20x Dall-Kirkham telescope (400 mm aperture) and transmitted into the atmosphere. The telescope is shared between the transmitter and the receiver. The telescope is mounted on a stepper motor, which enables elevation angle scanning capability. The polarization of the transmitted light pulses can be alternated, that allows a detection of oriented ice crystals.

The received light is focused by an apochromatic lens (EFL = 150 mm) into the field stop with an optical scrambler behind it. The optical scrambler is a 25mm long straight multimode optical fiber (300  $\mu$ m core), which homogenizes the intensity distribution of the received light. Then, the second apochromatic lens collimates the light, and the 1064 and 532 nm lidar returns are separated by a dichroic beamsplitter. The background noise from the sun is rejected by interference filters (0.35 nm FWHM @ 532 nm and 1nm FWHM @ 1064 nm) and Fabry-Perot etalons (FWHM=7.5 GHz, FSR=375 GHz, Tpeak = 76%, Fe = 49 @ 532nm, FWHM=7GHz, FSR=207 GHz, Tpeak = 94%, Fe = 28 @ 1064nm). The 532nm channels use pressure tuned Fabry-Perot etalons, and the 1064 nm channel has a solid etalon (fused silica glass) mounted in the temperature controlled kinematic mount. The etalon thickness is trimmed to match the etalon peak transmission at 30 C to the wavelength, corresponding to a doubled wavelength of the #1109 iodine absorption line.

The 20 % of the received signal in HSRL channel is reflected by 20/80 beamsplitter to the combined channel, which detects photons scattered by aerosols and molecules. The remaining portion of light passes through the narrow iodine filter (FWHM 1.8 GHz) where the aerosol signal is rejected. Then 28% of that light is reflected into the first molecular channel and the remaining light passes through the iodine filter with argon buffer

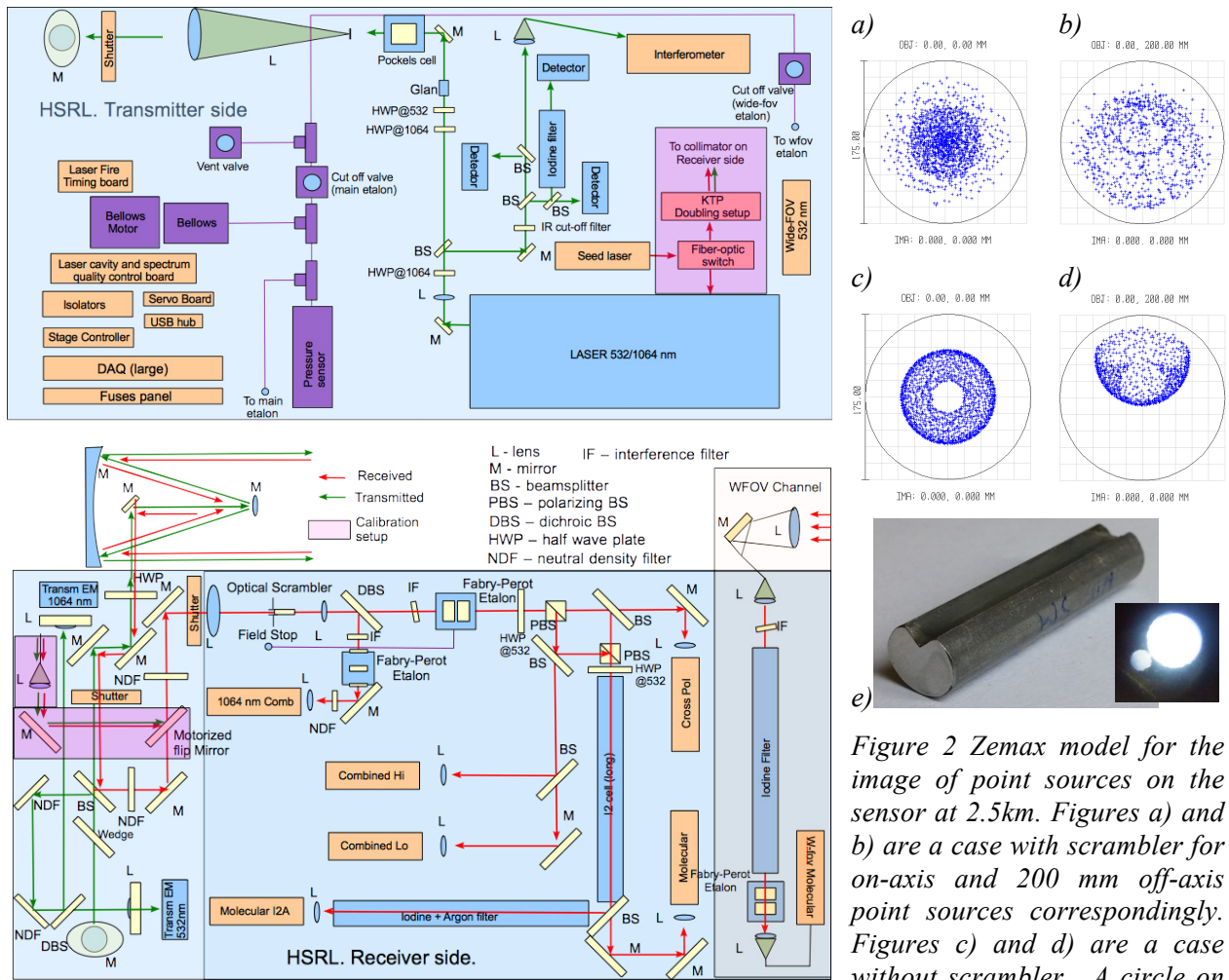


Figure 1 Schematic of the HSRL system: Top figure is the Transmitter side (bottom side of the optics breadboard); Bottom figure is the Receiver side (top side of the optics breadboard).

Figure 2 Zemax model for the image of point sources on the sensor at 2.5km. Figures a) and b) are a case with scrambler for on-axis and 200 mm off-axis point sources correspondingly. Figures c) and d) are a case without scrambler. A circle on the plots represents a 175  $\mu$ m sensor scale. Figure 2e is the photo of the optical scrambler.

gas (FWHM 2.85GHz). The second Iodine absorption filter buffered with Argon enables atmospheric temperature profile measurements. HSRL temperature profiling is described in work [2].

When the polarization switching is enabled, parallel and cross-polarized channels are alternated depending on the polarization state of transmitted light. Due to two polarization-splitting cubes in the receiver, molecular channels always receive 80% of the signal in any mode.

The instrument is also equipped with a wide-field-of-view (WFOV) channel at 532 nm. A WFOV folded telescope is mounted on the secondary mirror support structure of the large telescope and is coaxial with the transceiver. An aspherical lens

$f=100$  mm with  $f\#=2$  and a multimode fiber (105  $\mu$ m core) are used to construct that telescope. The fiber delivered signal is filtered with an interference filter, Fabry-Perot etalon with the same parameters as the main receiver and the iodine filter. The light is further coupled with a multimode fiber to the APD detector. The WFOV channel enables direct measurement of the instrument overlap function for the narrow-field-of-view channels. The measured overlap function is important for atmospheric extinction cross-section measurements.

### 2.3 Overlap function improvement for 1064nm channel

The HSRL instrument operates at two wavelengths and is capable of measuring volume backscatter coefficient and color ratio for 532 nm

and 1064 nm wavelengths. However, these measurements require accurate overlap functions for both wavelengths. In the previous instrument design each of the wavelengths had a separate field-stop, and, as a result, different overlap functions. Due to the difference in optics between the channels, that scheme caused large difference (up to 50%) in overlap functions between 532 and 1064 nm channels. In order to eliminate overlap function errors, we implemented apochromatic lenses and a shared field-stop in the receiver for all narrow-field-of-view channels.

## 2.4 Optical scrambling

The intensity distribution in the transmitted beam's cross-section is Gaussian. Due to a small field-of-view of the instrument, any shifts in the intensity distribution and possible non-uniform detector sensitivity across the sensor area appear in the signals as changes in the overlap function. Moreover, these changes can produce a difference in overlap functions between the channels sharing the same field stop. This is essential for atmospheric temperature profile measurements with HSRL [2]. In order to eliminate the differential overlap effect, we implemented a 25 mm long section of the multimode fiber (300  $\mu\text{m}$  core diameter) mounted behind the field-stop. The straight glass rod homogenizes the received beam by scrambling rays while preserving the polarization information in the signal. That allows the atmospheric depolarization coefficient measurements.

The multimode fiber is glued to a stainless steel rod with v-groove using a silicon rubber glue to avoid mechanical stress of the glass rod. In the first experimental samples we used epoxy, which caused stress and the polarization contrast decrease from 1:1000 (0.1%) to 40:100 (40%). With the silicon rubber glue the scrambler samples had depolarization as low as 2:1000 (.2%). For optics alignment purposes, a single mode fiber is glued in parallel to the multimode fiber. The single mode fiber has a length matching to the multimode one, and the fibers' axes skewness is around 200  $\mu\text{rad}$ . The scrambler is mounted on a translation stage so that when shifted laterally, in order to substitute the 3  $\mu\text{m}$  core single mode fiber for the 300  $\mu\text{m}$ , the fiber is used for lens collimation.

## 2.5 Calibration scans

The HSRL instrument uses an injection seeded Nd:YAG laser that produces two wavelengths. Originally, the seed laser operated in CW mode. After the laser firing, the seed laser light was amplified by the YAG crystal between the shots. This amplified light was saturating the IR channel detector. To avoid that, the seed laser was switched off after each laser shot and turned on around 80  $\mu\text{s}$  before the shot with simultaneous gating of the IR channel detector. That limited the maximum range of this channel and also produced a laser frequency chirp during the laser firing. In order to overcome these problems, a fast fiber-optic switch was added to the instrument. One of its outputs is connected to the host laser, and the second output is connected to the KTP assembly partially converting 1064 nm light into 532 nm. The multimode fiber delivers both wavelengths to the fiber collimator. A mirror mounted on the motorized flip mount directs the light to the receiver. That calibration setup is marked with pink boxes on Figure 1. For the instrument calibration, seed laser frequency scans across the receiver bandwidth are performed in order to measure the channels' transmission spectrum functions. The 95% duty cycle light pulses ( $\sim 237 \mu\text{s}$  pulse width) of the frequency doubled seed laser light (532nm) along with the large signal levels significantly improved the calibration accuracy. It decreased photon counting error by  $\sim 100$  times and the uncertainty in the laser output frequency. Previously, we used short  $\sim 50$  ns-wide pulses from the host laser at 4kHz pulse repetition rate. The newly measured channels' transmission functions do not require any adjustments for standard HSRL measurements.

## ACKNOWLEDGEMENTS

This work is supported by the Space Science and Engineering Center U. of Wisconsin – Madison.

## References

- [1] Eloranta, E. W.: High Spectral Resolution Lidar, in *Lidar: Range-Resolved Optical Remote Sensing of the Atmosphere*, Klaus Weitkamp ed., Springer, NY, pp. 25-30.
- [2] Razenkov Ilya et al, 2015: Atmospheric temperature profile measurements performed by the U. of Wisconsin – Madison High Spectral Resolution Lidar, *ILRC27*.